



Advanced Composite Materials

Publication details, including instructions for authors and subscription information:

<http://www.tandfonline.com/loi/tacm20>

Monitoring of electric conductance and delamination of CFRP using multiple electric potential measurements

Akira Todoroki^a

^a Department of Mechanical Sciences and Engineering, Tokyo Institute of Technology, 2-12-1 (i1-58) Ookayama, Meguro, Tokyo, 1528552, Japan.

Published online: 09 Oct 2013.

To cite this article: Akira Todoroki (2014) Monitoring of electric conductance and delamination of CFRP using multiple electric potential measurements, Advanced Composite Materials, 23:2, 179-193, DOI: [10.1080/09243046.2013.844900](https://doi.org/10.1080/09243046.2013.844900)

To link to this article: <http://dx.doi.org/10.1080/09243046.2013.844900>

PLEASE SCROLL DOWN FOR ARTICLE

Taylor & Francis makes every effort to ensure the accuracy of all the information (the "Content") contained in the publications on our platform. However, Taylor & Francis, our agents, and our licensors make no representations or warranties whatsoever as to the accuracy, completeness, or suitability for any purpose of the Content. Any opinions and views expressed in this publication are the opinions and views of the authors, and are not the views of or endorsed by Taylor & Francis. The accuracy of the Content should not be relied upon and should be independently verified with primary sources of information. Taylor and Francis shall not be liable for any losses, actions, claims, proceedings, demands, costs, expenses, damages, and other liabilities whatsoever or howsoever caused arising directly or indirectly in connection with, in relation to or arising out of the use of the Content.

This article may be used for research, teaching, and private study purposes. Any substantial or systematic reproduction, redistribution, reselling, loan, sub-licensing, systematic supply, or distribution in any form to anyone is expressly forbidden. Terms & Conditions of access and use can be found at <http://www.tandfonline.com/page/terms-and-conditions>

Monitoring of electric conductance and delamination of CFRP using multiple electric potential measurements

Akira Todoroki*

*Department of Mechanical Sciences and Engineering, Tokyo Institute of Technology,
2-12-1 (i1-58) Ookayama, Meguro, Tokyo 1528552, Japan*

(Received 24 April 2013; accepted 28 August 2013)

A new electrical potential method is proposed in the present study. Several electrodes to measure electric voltage are mounted on a carbon-fiber-reinforced-polymer beam surface. Direct current is applied and electric voltage changes are measured at each electrode. Comparing measured results with analytical results obtained from the anisotropic electric potential function, the electric conductance ratio can be obtained. Using this electric conductance ratio, the differences between the electric voltages on the surface are small and hence scaled to observe these variations. These differences in the electric potential enable the delamination location and delamination size to be determined. Uniform doublet analysis enables a relationship between the measured results and actual delamination location and delamination size to be established. The method is applied to some numerical analyses. A unidirectional carbon-fiber-reinforced polymer beam with a delamination crack is selected as a typical example encountered in analysis. The results show that the new method is quite effective for simple delamination crack monitoring.

Keywords: CFRP; electric conductance; electric potential; delamination; monitoring

1. Introduction

To detect delamination cracks within carbon-fiber-reinforced polymer (CFRP) composite laminates is difficult because such cracks are usually invisible. Difficulties in finding laminate damage by visual inspection raises the need of monitoring methods that use electric resistance changes within the laminates.[1–12] The method adopts conductive carbon fibers as sensors as well as mechanical reinforcements, that is, in a sense, self-sensing. The author's research group has proposed a method based on changes in electrical resistance to monitor location and size of the delamination [9,10]: several electrodes are placed on a target CFRP plate and changes in electrical resistance between these electrodes are measured. For the multiple-probe method, these changes in electric potential are measured at many locations; however, this method has a weak point in monitoring performance at the middle of electrodes where electric current is applied. A new two-way method has been proposed to improve monitoring performance.[11] To reduce experimental costs, an equivalent conductance that gives good agreement between FEM and experimental results has been obtained and FEM analyses have been used to obtain the relationship between the changes in electrical resistance

*Email: atodorok@ginza.mes.titech.ac.jp

and delamination.[12] These previous methods require electrical resistance or electric voltage measurements prior to delamination monitoring. With initial recorded measurement data for reference, differences from the reference data can be obtained during subsequent monitoring. Requiring reference data indicates that compensation must be performed to account for CFRP-conductance changes with environmental conditions such as temperature.[13] A new method that uses thermal deformation and electrical resistance change avoids the dependence on reference data.[14] The new method, however, does not monitor the exact location of damage.

The author has proposed an anisotropic electric potential function that assists the analysis of steady electric current within a CFRP laminate.[15,16] A new analytical method using a distributed anisotropic doublet enables the change in electric potential for a CFRP plate with a delamination crack to be calculated.[17] The method can be applied to a thin CFRP laminate using image analysis to obtain the electric current density.

For both the conventional electrical resistance change and electric potential change methods, electrical resistance or potential data are measured before damage has occurred, and the measured data are kept as a reference in subsequent damage monitoring of electrical resistance and electric potential changes. Nevertheless, compensation is indispensable to account for electric conductance changes caused by variation in temperature, moisture, and loading. Conductance values, moreover, have a large spread as a consequence of fabrication processes. This crucially means determining a compensation signature for each CFRP plate.

In the present study, a new monitoring method is proposed, beginning with a pre-identification of electric conductance for the CFRP plate, from which electric potential at the plate surface is calculated using the anisotropic electric potential function. Differences are then obtained between the calculated and measured electric voltage distributions. From differences in electric potential, delamination locations and their extent are simply determined based on a uniform-strength doublet theory. Numerical analyses of unidirectional CFRP are adopted to mitigate experimental errors. No limitation is placed on the number of measurement points; here, the theoretical performance of the delamination identification is investigated.

2. Delamination identification method

2.1. Monitoring method

A schematic representation of the new method is shown in Figure 1. The method comprises three steps. To avoid experimental errors for investigations of performance of the new method, we have opted for simulations of a CFRP beam using the finite difference method (FDM) instead of experiments. We assume that electric voltage can be measured at any point in the CFRP beam without limitation on the number of measurement points there.

In the first step, an electric current is applied to the CFRP beam surface from the outer pair of electrodes. Using the inner N electrodes, electric voltages are measured. The N electric voltage values are compared with the calculated electric voltage using image analysis,[17] using a conductance ratio $\lambda^2 = \sigma_z / \sigma_x$; here, σ_x is the conductance in the fiber direction and σ_z is the conductance in the thickness direction. A sum of squared errors is calculated for comparison. After changing the conductance ratio, the sum of squared errors is calculated, and the λ^2 that gives the minimum sum of squared errors is obtained. The value obtained is the conductance ratio of the CFRP beam.

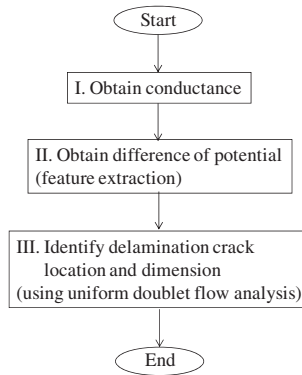


Figure 1. Monitoring flow chart for delamination and electric conductance.

In the second step, with this conductance ratio λ^2 , the electric potential of the CFRP surface is calculated using the anisotropic electric potential function. The calculated result is the electric potential for the delamination-free CFRP beam. The calculated result is set as the reference electric potential, and differences from this reference is measured at each electrode on the CFRP surface in measuring voltage changes. For this study, measurements are replaced by FDM calculations. The electric potential differences relative to the reference voltage are scaled up. These differences in electric potential over the CFRP surface include the features of electric potential for a delaminated CFRP beam.

In the third step, using the uniform-strength anisotropic doublet theory adopted here, delamination crack locations and their extents are identified. This method is detailed in the next section.

For the present study, unidirectional CFRPs of 0° -ply are simulated to simplify the FDM analysis. To deal with general laminated CFRPs that have various fiber directions, the analytical method is modified as described in [15,16]. The specific example adopted here is a unidirectional CFRP beam, 60-mm long and 3-mm thick, as illustrated in Figure 2; the spacing between electrodes is 30 mm. The nodes for the FDM mesh division are distributed 0.05 mm apart; the total number of nodes between the electrodes is 599. As mentioned before, the total number of electrodes used in measuring the electric voltage is maximized to reduce experimental errors; the number adopted is, therefore, 599. Figure 2 illustrates only a couple of electrodes where electric current is applied.

Here, the steady state electric current is computed using the FDM rather than commercial FEM analysis. Before starting the analysis, a simple FEM analysis using

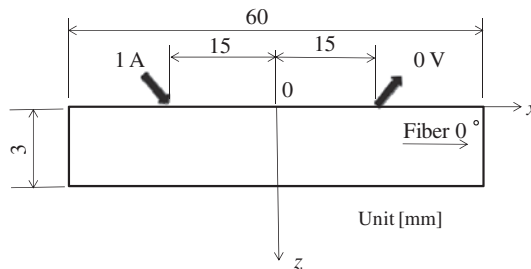


Figure 2. Specimen configuration.

ANSYS was performed; the FDM results were confirmed to provide identical results. In the FDM analysis, with node spacing in the z -direction of 0.005 mm, the total number of nodes is 721,801. Note, the mesh size is smaller in the z -direction than for the x -direction to make the mesh configuration square after an affine coordinate transformation. As described in detail in [15], the square root of the conductance ratio, $\lambda=0.1$, is taken to be the ratio of the affine coordinate transformation, which in turn determines the aspect ratio of the mesh. For the present study, the measured electric voltages are taken to be the results of the FDM calculations for the specimen surface. When actual experiments are conducted, the FDM analysis is replaced by the experimental results.

2.2. Identification of conductance using anisotropic electric potential function

As described in [17], the anisotropic electric potential function with the image analysis enabled us to calculate the electric current density of a thin CFRP laminate. That analysis provided excellent estimations of the electric current and electric voltage changes that compared favorably with the FEM results, even for thin CFRP laminates. The image analysis is very simple because the anisotropic electric potential function becomes a superposition of analytical formulas.

The image analyses of the anisotropic electric potential function are here performed with various conductance ratios λ^2 . Sum of squared errors of the measured N results compared with the image analysis are calculated and the conductance ratio that minimizes the sum of squared errors is searched. The electric potential at the electrodes where the electric current is applied, however, becomes infinite in the analysis, and the numerical computational error is larger at the electrodes compared with other nodes. Thus, the midpoint ($x=0$) between the electrodes is defined as the zero-point for the electric potential. The potential values for both electrodes are not included in the calculation of the sum of squared errors.

Figure 3 shows the electric potential distribution at the surface with various conductance ratios λ^2 . A commonly used conductance ratio is 0.01 for normal CFRP. More extreme conductance ratios, $\lambda^2=0.05$ and $\lambda^2=0.015$, are used here. An electric current of 1 A is applied in all cases. Figure 3 shows that a decrease in the conductance ratio brings about an increase in the electric potential between the electrodes.

Figure 4 shows the electric potential calculated using the FDM of $\lambda^2=0.0095$ that is slightly smaller than that of a normal CFRP. Although the results are not the

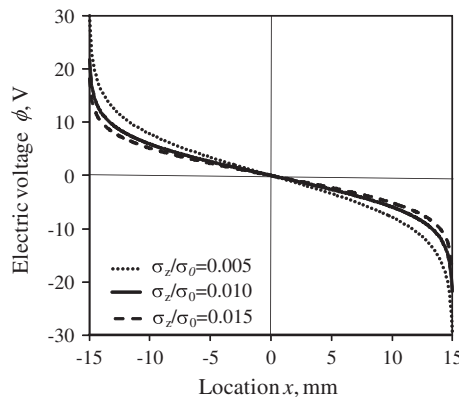


Figure 3. Surface variation of electric voltage due to electric conductance changes.

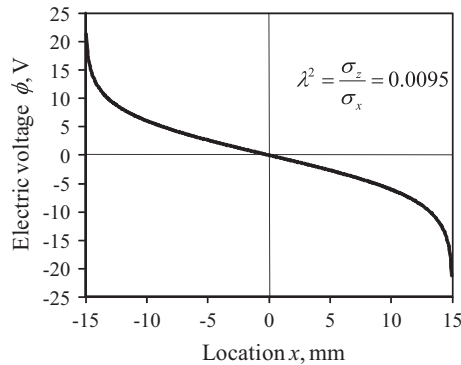


Figure 4. Surface variation of electric voltage at $\lambda^2 = 0.0095$.

experimental data, the results are treated as measured results in the present study to prevent experimental errors. The total number of measured points is 599, the same number of nodes as for the FDM with spacing 0.05 mm. Using various conductance ratios λ^2 , the surface electric potential distributions are calculated using the image analysis with the anisotropic electric potential function, and the sums of squared errors (Figure 5) for various electric conductance ratios, which are used for the image analysis with the anisotropic electric potential function. The minimum value of the sum of squared errors is obtained at $\lambda^2 = 0.0095$. Thus, the present method enables us to identify the electric conductance ratio of the measured thin CFRP. As the image analysis calculation is a simple superposition of the anisotropic electric potential, the computational cost is very low.

The dashed curve of Figure 6 presents the surface electric potential of a CFRP beam specimen with a 4-mm-long delamination at depth $z = 0.3$ mm ($\lambda^2 = 0.05$); the left tip of the delamination is located at $x_1 = -10$ mm and the right tip at $x_2 = -6$ mm. For comparison, the solid curve corresponds to the potential of a delamination-free beam surface; note that the difference between potentials is slight.

As for delamination-free beam specimen, the electric potential is measured at the points of 599 with spacing of 0.05 mm on the specimen surface between the electrodes. Using various conductance ratios λ^2 , image analyses of the anisotropic electric potential function are performed, and the sums of squared errors of various cases are calculated

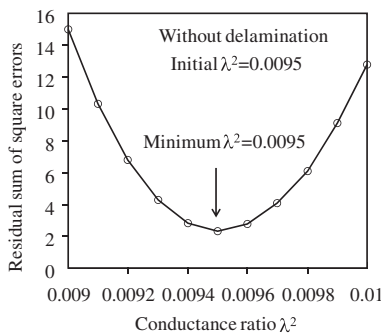


Figure 5. Identification of electric conductance using minimum residual sum of the squared errors of the intact specimen.

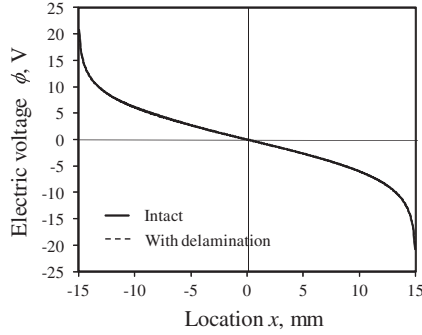


Figure 6. Surface electric voltage comparison of an intact specimen to one with delamination.

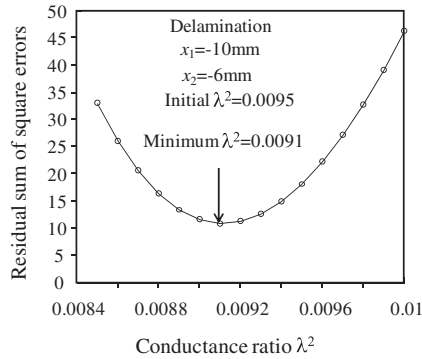


Figure 7. Identification of electric conductance using minimum residual sum of the squared errors of a specimen with delamination.

at all 599 points (see Figure 7). Clearly, a minimum value of the sum of squared errors is obtained at $\lambda^2 = 0.0091$ which is slightly different from the original conductance ratio. This difference is due to the presence of the delamination crack, but does not affect the measurements required in step 2.

Using the method described, the conductance ratios λ^2 obtained are almost the same as before monitoring. This means the monitoring process is not affected by changes in electric conductance caused by temperature or humidity changes. The method is also not affected by variances in the electric conductance established during fabrication. The method does not require a FEM analysis, and the method is easily extended to CFRP plates using a three-dimensional anisotropic electric potential function described in the reference based on the coupling approximation for angle plies.[15,16]

2.3. Feature extraction using difference of electric potential distributions

In step 1, the electric conductance ratio λ^2 of the CFRP is measured. Using the identified λ^2 , the electric potential of each point on the specimen surface can be calculated using image analysis of the anisotropic electric function: ϕ_{Ai} ($i = 1, \dots, N$). After the calculations, the difference ($\phi_{Mi} - \phi_{Ai}$) between the measured electric potential ϕ_{Mi} ($i = 1, \dots, N$) and the calculated electric potential ϕ_{Ai} ($i = 1, \dots, N$) is obtained, and the

difference is amplified to extract the feature of the electric potential difference. This is called differential amplification result.

Using the identified electric conductance ratio $\lambda^2=0.0091$, the electric potential of the specimen surface is calculated, and the differential amplification results are obtained. Figure 8 shows the differential amplification results of the specimen ($\lambda^2=0.0095$) with a 4-mm delamination crack ($x_1=-10$ mm, $x_2=-6$ mm); the dashed arrows mark the tip locations. From this figure, a local maximum value in the differential amplification is clearly observed. The meaning of the local maximum value is discussed next.

2.4. Delamination identification using uniform anisotropic doublet

The local maximum value of the differential amplification represents the effect of the delamination crack on the electric potential on the specimen surface. Here, the physical background is discussed using a uniform anisotropic doublet analysis.

As explained in [17], a change in the electric potential caused by the delamination crack is produced by a distributed doublet that is placed at the location of the crack; the doublet is placed to cancel the electric current flow perpendicular to the crack. Consider then a delamination crack existing at $z=z_0$ (the origin of the z -coordinate is on the specimen surface). To simplify the analytical formula, the z -coordinate is parameterized so that the crack is located at $z'=0$ in the new coordinates: $z'=z-z_0$. The doublet distribution μ is obtained by solving the integral equation,

$$i_z(x, z') = \frac{\sqrt{\sigma_z}}{2\pi} \int_{x_1}^{x_2} \mu(t) \frac{\left(\frac{x-t}{\sqrt{\sigma_x}}\right)^2 - \left(\frac{z'}{\sqrt{\sigma_z}}\right)^2}{\left\{\left(\frac{x-t}{\sqrt{\sigma_x}}\right)^2 + \left(\frac{z'}{\sqrt{\sigma_z}}\right)^2\right\}^2} dt, \quad (1)$$

where the left and right tips of the delamination crack are located at $(x_1, 0)$ and $(x_2, 0)$, respectively. The electric current density perpendicular to the crack surface is $i_z(x, 0)$ here. On the crack surface, $z'=0$, and this enables the current density from the integral equation to cancel i_z on the crack surface:

$$i_z(x, 0) = \frac{\sqrt{\sigma_z}}{2\pi\sigma_x} \int_{x_1}^{x_2} \frac{\mu(t)}{(x-t)^2} dt. \quad (2)$$

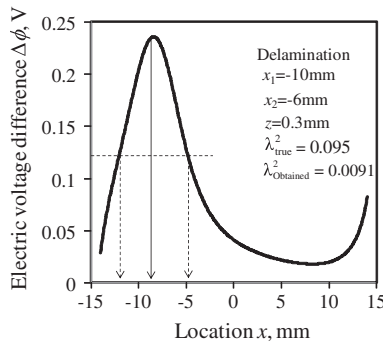


Figure 8. Electric voltage difference from the calculated voltage using the anisotropic electric potential function ($x_1 = -10$, $x_2 = -6$, $z = 0.3$).

Equation (2) is a hyper-singular integral equation that is not easy to solve analytically to get $\mu(x)$ exactly. Nevertheless, instead of setting $z'=0$, a small positive number ε is added to $z'=\varepsilon$ to prevent the hyper-singularity. The $i_z(x, 0)$ is used without a parallel shift of ε in the z -direction. This induces $z'=\varepsilon$ in Equation (1), and the hyper-singularity is removed. The change in the electric potential at the specimen surface after delamination is calculated by the distributed doublet $\mu(x)$.

To obtain $\mu(x)$, the integral equation must be solved with the given $i_z(x, 0)$. If the strength of the doublet is assumed to be uniform, the electric potential ϕ generated is given as follows,

$$\begin{aligned}\phi(x) &= -\frac{\mu}{2\pi} \int_{x_1}^{x_2} \frac{\frac{z_0}{\sqrt{\sigma_z}}}{\left(\frac{x-t}{\sqrt{\sigma_x}}\right)^2 + \left(\frac{z_0}{\sqrt{\sigma_z}}\right)^2} dt \\ &= -\frac{\mu}{2\pi} \left\{ \tan^{-1} \left(\frac{\frac{x_2-x}{\sqrt{\sigma_x}}}{\frac{z_0}{\sqrt{\sigma_z}}} \right) - \tan^{-1} \left(\frac{\frac{x_1-x}{\sqrt{\sigma_x}}}{\frac{z_0}{\sqrt{\sigma_z}}} \right) \right\}.\end{aligned}\quad (3)$$

Here, z_0 is the distance in the z -direction from the delamination crack to the specimen surface where the electric potential is measured. In Equation (3), $z_0 \gg \varepsilon$ must hold if ε is to be negligible.

As shown in [15], applying an affine coordinate transformation,

$$\zeta = \frac{x}{\sqrt{\sigma_x}}, \quad \eta = \frac{z}{\sqrt{\sigma_z}}, \quad (4)$$

To Equation (3) yields

$$\phi(x) = -\frac{\mu}{2\pi} \left\{ \tan^{-1} \left(\frac{\zeta_2 - \zeta}{\eta_0} \right) - \tan^{-1} \left(\frac{\zeta_1 - \zeta}{\eta_0} \right) \right\}, \quad (5)$$

where $\eta_0 = z_0/\sqrt{\sigma_z}$. If a parallel displacement is done in the ζ -coordinate to move the origin to the midpoint between the left tip ζ_1 and the right tip ζ_2 of the crack, i.e., introducing coordinate τ defined as,

$$\tau = \zeta - \frac{\zeta_1 + \zeta_2}{2}, \quad (6)$$

and substituting into Equation (6), Equation (5) becomes

$$\begin{aligned}\phi &= -\frac{\mu}{2\pi} \left\{ \tan^{-1} \left(-\frac{\tau}{\eta_0} + \frac{\zeta_2 - \zeta_1}{2\eta_0} \right) - \tan^{-1} \left(-\frac{\tau}{\eta_0} - \frac{\zeta_2 - \zeta_1}{2\eta_0} \right) \right\} \\ &= -\frac{\mu}{2\pi} \{ \tan^{-1}(\delta + \gamma) - \tan^{-1}(\delta - \gamma) \}\end{aligned}\quad (7)$$

where

$$\delta = \frac{\tau}{\eta_0}, \quad \gamma = \frac{\zeta_2 - \zeta_1}{2\eta_0}. \quad (8)$$

From Equation (7),

$$\begin{aligned}\frac{\partial \phi}{\partial \delta} &= -\frac{\mu}{2\pi} \left\{ \frac{1}{(\delta + \gamma)^2 + 1} - \frac{1}{(\delta - \gamma)^2 + 1} \right\} \\ &= -\frac{2\mu}{\pi} \frac{\delta \gamma}{\{(\delta + \gamma)^2 + 1\}\{(\delta - \gamma)^2 + 1\}}.\end{aligned}\quad (9)$$

Equation (9) indicates that the electric potential of the specimen surface has a local maximum value at $\delta=0$,

$$\delta = \frac{\tau}{\eta_0} = \frac{\xi - (\xi_1 + \xi_2)/2}{\eta_0} = 0 \quad \therefore \xi_m = \frac{\xi_1 + \xi_2}{2}, \quad x_m = \frac{x_1 + x_2}{2} \quad (10)$$

Thus, the differential amplification result has a local maximum value midpoint in the delamination crack.

The specimen's maximum surface potential ϕ_{\max} corresponding to the differential amplification result can be obtained by substituting $\delta=0$. Similarly, the specimen surface potential ϕ_γ for the differential amplification result at the delamination crack can be obtained by substituting $\delta=\pm\gamma$. A ratio α from these potentials $\alpha=\phi_\gamma/\phi_{\max}$ can be derived,

$$\alpha = \frac{\phi_\gamma}{\phi_{\max}} = \frac{\tan^{-1}(2\gamma)}{2 \tan^{-1}(\gamma)}, \quad (11)$$

the values of which clearly depend on γ (see Figure 9). Combining Equations (4) and (8), γ is expressible in the form

$$\gamma = \frac{\lambda(x_2 - x_1)}{2z_0}. \quad (12)$$

As indicated in Figure 9, but also obtainable from Equation (11), α asymptotes to 0.5 as γ becomes large. For a small delamination crack and a strongly orthotropic CFRP with very small conductance ratio λ^2 , the value of γ can be small. The extent of delamination, however, can be determined using $\alpha=0.5$ although this provides an overestimation, albeit a conservative estimate of crack length. Despite being an exact estimation,

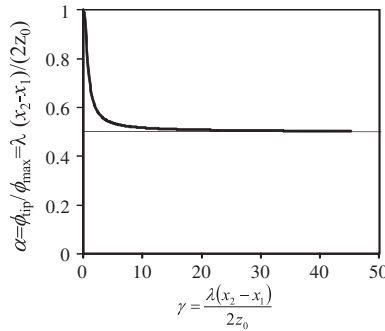


Figure 9. Ratio of the crack potential at the tip to that at the midpoint.

setting $\alpha=0.5$ gives a very simple method of estimating delamination crack length because $\alpha=0.5$ would mean the full-width-at-half-maximum of the differential amplification result gives the length of the delamination crack.

Summing up the method mentioned above, in the differential amplification results shown in Figure 8, the local maximum value is found at the center of the delamination crack, the full-width-at-half-maximum represents its length, and its location is at $x=-8$ mm. This corresponds to the exact estimation of the delamination location; the exact length is 6 mm and measured length is 4 mm. This method thus gives conservative estimates.

The electric current through the beam specimen as shown in Figure 2 flows downward on the left and upward on the right in returning to the electric ground electrode. The distribution of the electric current i_z at $z=0.3$ mm when $\lambda^2=0.01$ (see Figure 10) shows point symmetry with respect to the origin. This means that the differential amplification result has a local maximum if the delamination crack is located on the left side; in contrast, the differential amplification result has a local minimum if the delamination crack is located on the right side. If the delamination crack is located midpoint between the electrodes, the averaged i_z value is zero. This makes it difficult to detect this feature of the differential amplification result, as mentioned in Ref. [12]. This is discussed in the next section.

To investigate the effect of delamination depth, FDM calculations are performed for a delamination crack that is located along the x -axis as before but at a depth of $z=1$ mm. An electric conductance ratio of $\lambda^2=0.01$ is set. With the presence of the crack, an identified electric conductance ratio of $\lambda^2=0.0096$ is obtained, a value slightly different from the original. Using image analysis of the anisotropic electric potential function with the identified $\lambda^2=0.0096$, the electric potential of the specimen surface can be calculated. Compared with the calculated electric potential, the differential amplification result of the surface potential can be obtained, as shown in Figure 11. If a delamination crack develops far below the surface, the measured differential amplification result has a wider distribution because the uniform double exists at a deeper distance below the surface. Moreover, the maximum value of the local maximum value is smaller than the result for a shallow delamination crack. The delamination location determined from the maximum point is -5.8 mm, with left tip at $x_1=-7.8$ mm and right tip at $x_2=-2.4$ mm yielding a crack length of 5.4 mm. With an actual length of 4 mm, the difference is not so significant. Because the differential amplification result is less precise for deep delamination cracks, the monitoring performance worsens but the estimates remain conservative.

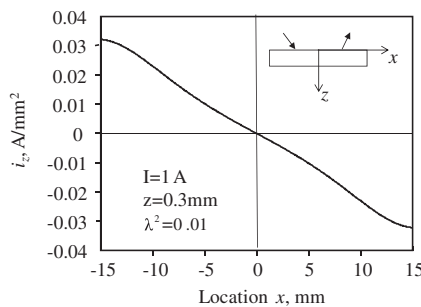


Figure 10. Electric current density in the z -direction at $z=0.3$ mm.

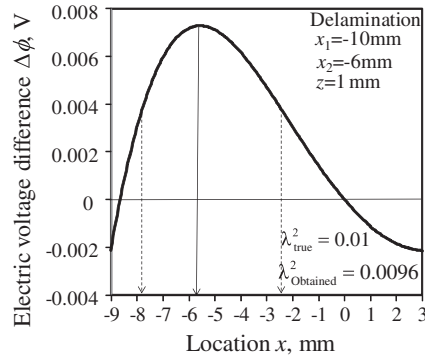


Figure 11. Electric voltage difference from the calculated voltage using the anisotropic electric potential function ($x_1 = -10$, $x_2 = -6$, $z = 1.0$).

Let us consider the number of measurements on the surface to extract the feature of the differential amplification result. In the present study, electrode spacing is set to 0.05 mm corresponding to FDM grid division. From a practical point of view, the total number of measurement points should be reduced.

As stated earlier, the delamination length can be identified from the full-width-at-half-maximum of the measured differential amplification result. This means that the required electrode spacing is determined when the minimum target length of the delamination crack is determined. If an approximate local maximum point is calculated using a quadratic polynomial, three points at least are required. This means that the required electrode spacing is one-third of the minimum target length of a delamination crack. For example, if a delamination crack of 7 mm is the target minimum length, the required minimum electrode spacing is 2 mm. More experimental investigation will be undertaken on this aspect in future work.

3. Identification of the center crack between electrodes

If a delamination crack occurs midpoint between the electrodes where electric current is applied, the electric current density perpendicular to the crack at the center vanishes, whereas on either side it has the same magnitude but opposite sign; the electric current has point-symmetry with respect to the center point. As the electric current density is continuous, the electric current magnitude is very small. Consider Figure 2 where a delamination crack is present along the centerline in the specimen. In this case, we can consider that two cracks to be the same length left and right of center: the left crack is located from $x_1 = -x_0$ to 0 ($x_0 > 0$) and the right crack from 0 to $x_2 = x_0$. As the electric current distribution is anti-symmetric about the origin, each doublet has the same strength but opposite sign. From Equation (5), the effect of twin doublets of different sign is given in Figure 12, and shows the surface electric potential distribution normalized by the strength of the doublet $\mu/(2\pi)$; settings for the calculation are $x_0 = 2$ mm, depth $z_0 = 0.2$ mm, and $\lambda^2 = 0.01$. If a delamination crack is present midpoint between the electrodes, the measured electric potential is characterized by a convex-concave function, as shown in Figure 12. The magnitude is, however, very small because of the small doublet strength generated by the small i_z .

Let us consider a delamination crack of 4 mm length as before but at a depth of $z_0 = 0.3$ mm. The identified electric conductance is $\lambda^2 = 0.098$. An image analysis of the

anisotropic electric potential with the identified λ^2 is performed; the differential amplification result obtained exhibits a minute concave–convex variation (marked by arrows in (Figure 13)). These two points are assumed to be a pair of twin doublets.

The surface electric potential of the left delamination crack can be obtained by substituting $\xi_2=0$ into Equation (5). In the calculation, $\xi_1 = -\xi_0 = -x_0/\sqrt{\sigma_x}$; $2x_0$ is equal to the delamination crack length

$$f_L = \frac{2\pi}{\mu} \phi(x) = -\tan^{-1}\left(\frac{\xi}{\eta_0}\right) + \tan^{-1}\left(\frac{\xi + \xi_0}{\eta_0}\right). \quad (13)$$

Similarly, the surface electric potential of the right delamination crack can be obtained by substituting $\xi_1=0$ into Equation (5). Considering the odd parity of the doublet strength, the electric potential is obtained as follows,

$$f_R = \frac{2\pi}{\mu} \phi(x) = -\tan^{-1}\left(\frac{\xi}{\eta_0}\right) + \tan^{-1}\left(\frac{\xi - \xi_0}{\eta_0}\right). \quad (14)$$

Using parameterizations $\tau = \xi/\eta_0$ and $\tau_0 = \xi_0/\eta_0$, the total sum of the twin doublet is

$$f = f_L + f_R = -2 \tan^{-1}(\tau) + \tan^{-1}(\tau + \tau_0) + \tan^{-1}(\tau - \tau_0), \quad (15)$$

From which the extremum of the normalized surface potential τ_m can be obtained; that is,

$$\frac{\partial f}{\partial \tau} = -\frac{2}{\tau^2 + 1} + \frac{1}{(\tau + \tau_0)^2 + 1} + \frac{1}{(\tau - \tau_0)^2 + 1} = 0, \quad (16)$$

yields

$$\tau_m = \pm \sqrt{\frac{\tau_0^2 + 1}{3}}, \quad (17)$$

$$\therefore x_m = \pm \sqrt{\frac{x_0^2 + z_0^2/\lambda^2}{3}}. \quad (18)$$

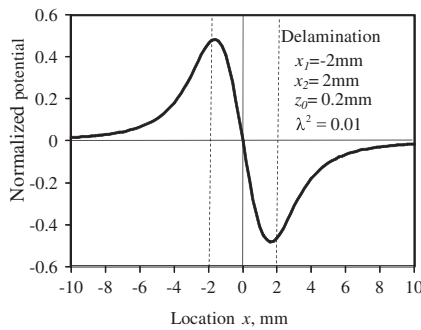


Figure 12. Normalized potential distribution for a delamination located midpoint between the electric current electrodes.

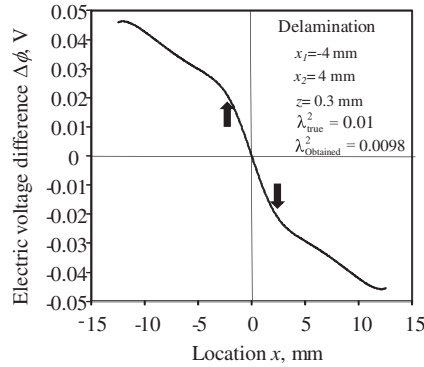


Figure 13. Electric voltage difference from the calculated voltage using the anisotropic electric potential function ($x_1 = -28$, $x_2 = -32$, $z = 0.3$).

From Equation (18), the delamination crack length $2x_0$ is then

$$2x_0 = 2\sqrt{3x_m^2 - \frac{z_0^2}{\lambda^2}}. \quad (19)$$

Although the depth of the delamination z_0 is unknown, the minimum expected value is clearly the thickness of a ply (e.g. 0.125 mm). This minimum expected value gives a conservative estimate of the delamination crack length. Using the measured value of $x_m = 2$ mm from Figure 12, $\lambda^2 = 0.098$ and the conservative value of $z_0 = 0.125$ mm, the conservative estimate of the delamination length is then $2x_0 = 6.4$ mm slightly above the actual value of 4 mm.

As shown here, even if a delamination crack exists midpoint between the electrodes where electric current is applied, the differential amplification result features a characteristic concave–convex curve. From the extremum of the sine wave, a conservative delamination crack length is estimated using Equation (19). The magnitude of the characteristic concave–convex sine wave is, however, very small because of the small electric current density across the CFRP plate. Experimental performance will be taken up in future work.

For a delamination crack at the center, the electric potential method was shown in [11] to be experimentally unsuitable. From the experimental results, the characteristic concave–convex curve of the differential amplification result was not obtained. In this instance, another electrode pair can be used to apply a second electric current. In the second case, the center for the electrodes is moved to a different point. Using this two-way method described in [11], the electric potential method performs well. The same method can be applied in this case.

4. Conclusions

A new monitoring method was proposed here. Using multiple point electrodes, the electric potential distribution of a CFRP beam can be measured. Image analysis using the anisotropic electric potential function identified the electric conductance ratio from which the characteristic differential amplification result can be obtained. From the

extremum of the result, delamination location and length were determined. The results obtained are as follows:

- (1) From the electric potential distribution on the surface of a CFRP specimen, the electric conductance ratio can be identified. This enables delamination cracks to be monitored without the need to consider temperature and humidity changes.
- (2) It is possible to obtain characteristic electric potential distribution from the differential amplification result using the calculated electric potential with the anisotropic electric potential function.
- (3) The location of the center of the delamination crack can be obtained from the location of the extremum of the measured differential amplification result, while delamination length can be obtained from the full-width-at-half-maximum of the differential amplification result. The method gives conservative estimates of the crack length; good estimates are obtained for cracks at shallow depths, but slight overestimates were obtained for cracks deeper beneath the surface.
- (4) If a delamination crack is present midpoint between the electrodes, the characteristic differential amplification result of a concave–convex sine wave is observed. From the position of the extremum, the delamination crack length can be obtained. The output of the concave–convex sine wave is, however, very small.

References

- [1] Schulte K, Baron CH. Load and failure analyses of CFRP laminates by means of electrical resistivity measurements. *Compos. Sci. Technol.* 1989;36:63–76.
- [2] Muto N, Yanagida H, Nakatsuji T, Sugita M, Ohtsuka Y. Preventing fatal fractures in carbon-fibre–glass-fibre-reinforced plastic composites by monitoring change in electrical resistance. *J. Am. Ceram. Soc.* 1993;76:875–879.
- [3] Wang X, Chung DDL. Continuous carbon fibre epoxy-matrix composite as a sensor of its own strain. *Smart Mater. Struct.* 1996;5:796–800.
- [4] Irving PE, Thiagarajan C. Fatigue damage characterization in carbon fibre composite materials using an electrical potential technique. *Smart Mater. Struct.* 1998;7:456–466.
- [5] Seo DC, Lee JJ. Damage detection of CFRP laminates using Electrical resistance measurement and a neural network. *Compos. Struct.* 1999;47:525–530.
- [6] Abry JC, Choi YK, Chateauminois A, Dalloz B, Giraud G, Salvia M. In-situ monitoring of damage in CFRP Laminates by using AC and DC measurements. *Compos. Sci. Technol.* 2001;61:855–864.
- [7] Park JB, Okabe T, Takeda N, Curtin WA. Electromechanical modeling of unidirectional CFRP composites under tensile loading condition. *Compos. Part A.* 2002;33:267–275.
- [8] Ogi K, Takao Y. Characterization of piezoresistance behavior in a CFRP unidirectional laminate. *Compos. Sci. Technol.* 2005;65:231–239.
- [9] Todoroki A, Tanaka Y. Delamination identification of cross-ply graphite/epoxy composite beams using electric resistance change method. *Compos. Sci. Technol.* 2002;62:629–639.
- [10] Todoroki A, Tanaka M, Shimamura Y. Measurement of orthotropic electric conductance of CFRP laminates and analysis of the effect on delamination monitoring with electric resistance change method. *Compos. Sci. Technol.* 2002;62:619–628.
- [11] Ueda M, Todoroki A. Asymmetrical dual charge EPCM for delamination monitoring of CFRP laminate. *Key Eng. Mater.* 2006;321–323:1309–1315.
- [12] Ueda M, Todoroki A. Delamination monitoring of CFRP laminate using the two-stage electric potential change method with equivalent electric conductivity. *Eng. Fract. Mech.* 2008;75:2737–2750.
- [13] Todoroki A, Tanaka Y, Shimamura Y. Electric resistance change method for identification of embedded delamination of CFRP plates. *Mater. Sci. Res. Int.* 2001;139–145, Special Technical Publication-2, JSMS.

- [14] Suzuki Y, Todoroki A, Matsuzaki R, Mizutani Y. Impact damage visualization in CFRP by resistive heating: development of a new detection method for indentations caused by impact loads. *Compos. Part A*. 2012;43:53–64.
- [15] Todoroki A. Electric current analysis of CFRP using perfect fluid potential flow. *Trans. Jpn Soc. Aero. Space Sci.* 2012;55:183–190.
- [16] Todoroki A. Electric current analysis for thick laminated CFRP composites. *Trans. Jpn Soc. Aero. Space Sci.* 2012;55:237–257.
- [17] Todoroki A, Arai M. Simple electric-voltage-change-analysis method for delamination of thin CFRP laminates using anisotropic electric potential function. *Adv. Compos. Mater.* (in press).